Article

Redox Transformations of Arsenic and Iron in Water Treatment Sludge during Aging and TCLP Extraction

Xiaoguang Meng, George P. Korfiatis, Chuanyong Jing, and Christos Christodoulatos

Environ. Sci. Technol., **2001**, 35 (17), 3476-3481• DOI: 10.1021/es010645e • Publication Date (Web): 27 July 2001

Environ. Sci. Technol. **2001**, *35,* 3476−3481

Redox Transformations of Arsenic and Iron in Water Treatment Sludge during Aging and TCLP Extraction

XIAOGUANG MENG,*
GEORGE P. KORFIATIS,
CHUANYONG JING, AND
CHRISTOS CHRISTODOULATOS

Center for Environmental Engineering, Stevens Institute of Technology, Hoboken, New Jersey 07030

Laboratory experiments and modeling studies were performed to investigate the redox transformations of arsenic and iron in water treatment sludge during aging, and to evaluate the impact of those transformations on the leachability of arsenic determined with the U.S. EPA toxicity characteristic leaching procedure (TCLP). When the backwash suspension samples collected from a California surface water treatment plant were aged in closed containers for a few weeks, soluble arsenic increased from less than 5 μg/L to as high as 700 μg/L and then decreased dramatically because of biotic reduction of arsenate [As(V)], ferric oxyhydroxide, and sulfate. The experimental results and the thermodynamic models showed that arsenic mobility can be divided into three redox zones: (a) an adsorption zone at pe > 0, which is characterized by strong adsorption of As(V) on ferric oxyhydroxide; (b) a mobilization (transition) zone at $-4.0 <$ pe < 0, where arsenic is released because of reduction of ferric oxyhydroxide to ferrous iron and As(V) to arsenite [As(III)]; and (c) a reductive fixation zone at pe < -4.0, where arsenic is immobilized by pyrite and other reduced solid phases. The TCLP substantially underestimated the leachability of arsenic in the anoxic sludge collected from sludge ponds because of the oxidation of Fe(II) and As(III) by oxygen. The leaching test should be performed in zero-headspace vessels or under nitrogen to minimize the transformations of the redox-sensitive chemical species.

Introduction

Coagulation treatment with ferric chloride is commonly used for the removal of arsenic from water (*1*−*3*). The more stringent maximum contaminant level (MCL) of 3 to 20 μg/L arsenic currently under consideration by the U.S. EPA (*4*) will require thousands of water treatment facilities in the U.S. to install new arsenic removal processes, or to upgrade existing processes. As a result, millions of tons of arsenic-bearing sludge will be generated annually from such water treatment processes (*5*). Accurate measurement and prediction of arsenic leachability from these sludges is crucial to the selection of proper disposal options, which range in cost from less than $50 per ton for nonhazardous sludge to a few hundred dollars per ton for hazardous material.

As(V) and As(III) are the predominant inorganic arsenic species in surface water and groundwater (*6*). Because As(III) has a weaker affinity for ferric hydroxides than As(V) in a neutral pH range, it is usually oxidized to As(V) prior to the coagulation treatment in order to improve the efficiency of arsenic removal. Therefore, most of the arsenic in the fresh sludge generated in the water treatment processes should be present as As(V). When the sludge is disposed of in a lagoon or a landfill, As(V) and Fe(III) may be reduced to As(III) and soluble Fe(II), respectively, resulting in the release of arsenic into the surrounding environment. Dissimilatory As(V)-reducing microorganisms have been identified in aquatic sediments (*7, 8*). In addition, the reductive dissolution of iron oxhydroxide by iron-reducing bacteria may contribute significantly to the release of adsorbed arsenic and dissolution of arsenic minerals in the sediments (*9, 10*). As(V) can be reduced by sulfide formed through microbially mediated sulfate reduction in the sediments (*11*−*13*). In contrast to reductive arsenic release, immobilization of arsenic can be achieved through the formation of various minerals with sulfide and ferrous in anoxic environments (*14*).

The disposal of wastes is regulated by the U.S. EPA and state agencies according to the leaching potential of pollutants determined by standard extraction tests. The toxicity characteristic leaching procedure (TCLP) is the most commonly used regulatory protocol (*15, 16*). The test is performed by tumble mixing a waste sample with a dilute acetic acid solution at a liquid-to-solid ratio of 20 for 18 h. For the extraction of nonvolatile species such as arsenic, the method does not require a zero-headspace in the extraction vessel or the exclusion of oxygen from the extraction system. Redox-sensitive chemical species such as As(III) and Fe(II) in the samples may be oxidized during the extraction test, resulting in the adsorption of As(V) on precipitated ferric oxyhydroxide. Thus, the TCLP may underestimate the potential for arsenic release from sludge in anoxic environments.

In the present study, reductive transformations of As(V) and ferric oxyhydroxide in water treatment sludge were evaluated by conducting aging experiments and applying a chemical equilibrium model. The effects of dissolved oxygen on the TCLP leachability of arsenic in the sludge were tested in separate experiments. The findings of the present study are important for the understanding of arsenic mobility in sludge generated by water treatment facilities, as well as in natural sediments and soils under various redox conditions.

Materials and Methods

Water Treatment Sludge and Suspension Samples. A water treatment plant in California provided sludge and suspension samples generated from the treatment of surface water. Arsenic in the source water is removed by coprecipitation with ferric chloride (at doses between 0.6 and 1.6 mg/L) followed by a sand filtration (*17, 18*). Cationic polymer coagulant (Cytec Superfloc C-592) and ozone are also added to the source water prior to filtration. The average arsenic concentration in the source water is approximately 10 μg/L. The direct filtration process removes between 30 and 60% of the arsenic. The backwash suspension is discharged into sludge ponds for de-watering. It takes approximately two years to achieve sufficient water removal prior to the disposal of the solids at designated sites.

Sludge samples were collected from Ponds 3 and 5 after the sludge had been accumulated in the ponds for approximately one year. Fresh suspension samples were collected in a 40-gallon container during the backwash cycle of the sand filters. After the solids settled for 2 to 4 h, the thickened suspension was transferred into a 5-gallon collapsible polyethylene container and shipped to our laboratory

* Corresponding author phone: (201) 216-8014; fax: (201) 216-8303; e-mail: xmeng@stevens-tech.edu.

10.1021/es010645e CCC: $20.00
Published on Web 07/27/2001

TABLE 1. Characteristics of the Sludge and Suspension Samples

	pH	solid content (g/100 g sample)	total As (mg/kg solid)	total Fe (g/kg solid)	extractable Fe(II) (%)
suspension 1 (S-1)	7.15	3.4	638	84.8	NA
suspension 2 (S-2)	6.98	0.8	794	81.5	NA
pond 3 sludge	5.35	22	1540	122	38
pond 5 sludge	6.96	17	935	93.5	57

overnight. The suspension samples were collected in February and October 2000. Supernatant samples were collected from the 40-gallon container during the settling and were filtered through a 0.4-μm membrane and then through an arsenic-speciation cartridge for the determination of particulate and soluble As(V) and As(III). The sludge and suspension samples (1.00 g) were acid digested using 1:1 HNO_3, concentrated HNO_3, and 30% H_2O_2 repeatedly on a hot plate to dissolve iron oxyhydroxide (*19*). After the digested samples cooled, they were diluted to 100 mL with DI water for analysis of total As and Fe by furnace atomic absorption spectrometry (AAS) and inductively coupled plasma (ICP) emission spectrometry, respectively.

Aging Test of Suspension Samples. Reductive transformations of As(V) and ferric oxyhydroxide were evaluated by aging the backwash suspension samples in the collapsible plastic containers in the dark, at room temperature. Most of the headspace air was extruded from the containers before the aging tests. Aliquots of suspension samples were periodically withdrawn from the containers during approximately 80 days of testing. The samples were filtered immediately through a 0.4-μm membrane and arsenic-speciation cartridges for analyses of soluble As(V), As(III), Fe, and sulfate. The pe (pe $= -\log\{e^-\}$, where $\{e^-\}$ represents the electron activity), pH, and dissolved oxygen (DO) content of the suspension samples were also monitored during the aging period.

A combined Pt−Ag/AgCl redox electrode (4 M KCl) (Orion 96-78) was connected to a pH/millivolt meter (Orion 611) for the measurement of E_H (the redox potential). Prior to every E_H measurement, calibrations were carried out using the Zobell's solution (3×10^{-3} M potassium ferrocyanide and 3×10^{-3} M potassium ferricyanide in 0.1 M KCl) with a standard potential of +228 mV at 25 °C. After the electrode was rinsed with DI water and then with the sample, it was placed in the sample for E_H measurement. The sample, in a 50-mL beaker, was mixed gently under N_2 during E_H measurement.

Leaching Tests. The TCLP tests were conducted by mixing pond sludge samples or filter cake from the fresh suspension with the TCLP leachant in capped polypropylene bottles. The fresh suspension was filtered through a 0.4-μm membrane to collect the filter cake for the TCLP testing. In accordance with the TCLP protocol (*15*), the sludge samples were extracted with TCLP leachant containing 0.10 M acetic acid and 0.064 M NaOH (pH = 4.93) at a leachant-to-sludge mass ratio of 20. After 18 h of mixing, the extraction solution was separated from the solid by filtration and analyzed for soluble arsenic and iron.

The effect of oxygen on the amount of arsenic extracted by the TCLP was evaluated by conducting three modified TCLP experiments. In the first test, mixtures of the sludge sample and the leachant in the extraction vessels were purged with nitrogen gas for 15 min prior to the TCLP test. The second experiment was conducted by varying the headspace-to-leachant volume ratio (V_a/V_l) at a fixed leachant-to-sludge ratio of 20. Because the TCLP protocol does not specify the size of the extraction vessels, bottles of different sizes were used during the extraction tests to provide V_a/V_l ratios of 0.1, 0.5, and 1.25. Finally, a kinetic experiment was carried out by mixing the sludge samples with the TCLP leachant in beakers with a magnetic mixer. The beakers were open to the air or purged with nitrogen gas during the mixing. Aliquots of suspension samples were withdrawn at desirable time intervals and analyzed for soluble As and Fe.

Speciation of As and Fe. As(V) and As(III) in the water samples were separated with arsenic-speciation cartridges (Metalsoft Center, Highland Park, NJ) (*20*, *21*). The cartridges packed with 2.5 g of aluminosilicate adsorbent selectively removed As(V) but did not adsorb As(III) in a pH range 4 to 9. As(III) was separated from As(V) by passing approximately 50 mL of sample through a cartridge at a flow rate of 60 ± 30 mL per minute using a syringe. Before the leachate samples obtained in the TCLP tests were passed through the cartridges, they were diluted 10 times with DI water to eliminate the interference of acetate with the As(V) removal. Spike and recovery tests on a representative range of samples indicated that the cartridges removed more than 98% of the As(V) and less than 5% of the As(III).

The Fe(II) in the sludge samples was extracted with 0.5 M HCl at a liquid-to-solid ratio of 10 (*22*). The mixture was purged with nitrogen gas for 15 min and then mixed in capped containers for 24 h. After separation of the solids by filtration, the soluble or extractable Fe(II) was immediately measured by the phenanthroline method (*23*). The total soluble Fe concentration was determined by ICP. The amount of ferric oxyhydroxide in the backwash suspensions during the aging test was calculated by subtracting the soluble Fe and solid-phase Fe(II) from the total Fe content.

Results and Discussion

Release of Arsenic and Iron during Aging. The physical and chemical properties of the suspension and sludge samples are summarized in Table 1. The arsenic content in the samples ranged from 638 to 1540 mg/kg of dry solids. The suspension samples contained 0.8 and 3.4% solids, whereas the solids content in the sludge samples was 17 and 22%. The variations in the arsenic and iron content were attributed to different arsenic concentrations in the source water and different ferric chloride doses used in the water treatment process.

The total soluble arsenic concentration in the fresh Suspension 1 (sample S-1) was approximately 1.5 μg/L. No soluble As(III) was detected in the suspension. This was expected because the source water was from a reservoir and was treated with ozone prior to the sand filtration. The soluble iron concentration in sample S-1 was 27 μg/L. After the suspension was aged for 2 days in the closed container, the soluble As(III) and Fe concentrations increased slightly to 5.6 μg/L and 45 μg/L, respectively. No increase in the soluble As(V) concentration was observed. The dissolved oxygen was reduced to less 0.5 mg/L in the suspension. These results indicated that anoxic conditions were rapidly established in the suspension samples because of biological activity.

The changes in soluble arsenic and iron concentrations during approximately 80 days of aging are shown in Figure 1. The formation rate of soluble As(III) and Fe was low in the first 3 days, representing a lag period. Thermodynamic calculations using the computer program MINTEQA2 (*24*) indicated that in the neutral pH range the reduction of DO, As(V), and ferric oxyhydroxide [FeOOH(am)] would occur at

TABLE 2. Reactions and Parameters Used in the Model Calculations

surface reactions	equilibrium expressions	log K
1. Model Suspension 2 (S-2) System (initial total contents)		
Fe(III) = 12 mM (672 mg/L)		
As(V) = 0.085 mM (6.38 mg/L)		
SO_4^{2-} = 0.417 mM (40.0 mg/L)		
HCO_3^- = 2.32 mM (141.5 mg/L)		
Ionic strength I = 0.04 M (as KNO_3), pH = 7.0		
2. Surface Parameters and Reactions		
[a]Surface site (SOH) density = 0.9 mmol/1 mmol Fe		
C_1 = 140 μF/cm^2; C_2 = 20 μF/cm^2		
(1) $SOH + H_3AsO_4 = SAsO_4^{2-} + H_2O + 2H^+$	$K = \exp(-2F\psi_0/RT)[SAsO_4^{2-}][H^+]^2/[SOH][H_3AsO_4]$	−2.3[b]
(2) $SOH + H_3AsO_3 = SHAsO_3^- + H_2O + H^+$	$K = \exp(-F\psi_0/RT)[SHAsO_3^-][H^+]/[SOH][H_3AsO_3]$	−3.3[b]
(3) $SOH + H^+ = SOH_2^+$	$K_{a1} = \exp(F\psi_0/RT)[SOH_2^+]/[SOH][H^+]$	5.1[a]
(4) $SOH = SO^- + H^+$	$K_{a2} = \exp(-F\psi_0/RT)[SO^-][H^+]/[SOH]$	−10.7[a]
(5) $SOH + K^+ = SO - K + H^+$	$K_K = \exp(F(\psi_\beta - \psi_0)/RT)[SO - K][H^+]/[SOH][K^+]$	−9.0[a]
(6) $SOH + NO_3^- + H^+ = SOH_2 - NO_3$	$K_{NO3} = \exp(F(\psi_0 - \psi_\beta)/RT)[SOH_2 - NO_3]/[SOH][H^+][NO_3^-]$	6.9[a]
3. Redox Reactions		
(7) $H_3AsO_4 + 2H^+ + 2e^- = H_3AsO_3 + 2\,H_2O$		18.9[c]
(8) $Fe^{3+} + e^- = Fe^{2+}$		13.0[c]
(9) $SO_4^{2-} + 9H^+ + 8e^- = HS^- + 4H_2O$		33.7[c]
4. Precipitation Reactions		
(10) $Fe^{3+} + 2H_2O = FeOOH(am) + 3H^+$		−2.5[d]
(11) $Fe^{2+} + CO_3^{2-} = FeCO_3$ (siderite)		10.2[c]
(12) $2H_3AsO_3 + 3HS^- + 3H^+ = 6H_2O + As_2S_3$ (orpiment)		61.1[c]
(13) $Fe^{2+} + 2HS^- = 2H^+ + 2e^- + FeS_2$ (pyrite)		18.5[c]

[a] From Meng et al. (*21*). [b] Best-fit constants determined with model simulations of the experimental data. [c] From MINTEQA2 database (*24*). [d] From Stumm and Morgan (*30*).

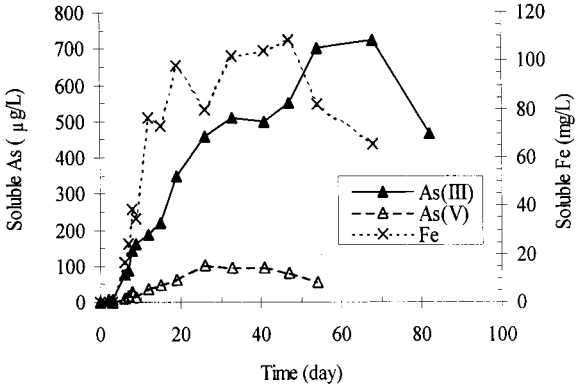

FIGURE 1. Release of As and Fe during aging of Suspension 1 (S-1) sample in a closed system. Suspension pH during aging: 7.15−7.47.

pe values of approximately 13, 1, and −1, respectively. In the initial aging period, DO was consumed by the aerobic microorganisms. As the redox potential further decreased, As(V) and FeOOH(am) were reduced to more mobile As(III) and Fe(II). Meng et al. (*21*) have shown that at low total As(III) concentrations, most of the As(III) is adsorbed on the ferric oxyhydroxide particles. Therefore, adsorption of As(III) on the solid surface could further extend the lag time in addition to that required for the depletion of DO.

When the aging time increased from 3 to 60 days, the soluble As(III) and Fe concentrations increased substantially (Figure 1). The soluble concentrations of As(III) and Fe reached maximum values of 700 μg/L (at day 60) and 100 mg/L (at day 45), respectively. After 26 days of aging, the soluble As(V) concentration increased gradually to approximately 100 μg/L. The release of As(V) could be caused by the dissolution of ferric oxyhydroxide. When the aging time was longer than approximately 50 days, the soluble As and Fe concentrations began to decrease. It should be noted that the changes in the As(V) and As(III) concentrations followed a pattern similar to that of Fe. The pH of the suspension increased slightly from 7.15 to 7.41 during the aging period.

Modeling Transformations of As, S, and Fe during Aging. The thermodynamic constants for the precipitation and reduction of As, Fe, and S species are well established. However, the adsorption constants of solutes such as As(V) and As(III) vary with the adsorption systems and types of surface adsorption models (*25*, *26*). The triple layer model (TLM) has been used to simulate the adsorption of As(V) and As(III) on pure ferric oxyhydroxide in a KNO_3 solution (*21*). The adsorption constants obtained in this system could not be used to describe the adsorption isotherms in the backwash suspensions because of the effects of coexisting anions and the interactions of ferric oxyhydroxide with other inorganic and organic particles in the suspension.

In the present work, the adsorption constants for As(V) and As(III) in the fresh suspensions were estimated by fitting the TLM to the experimental data. The other surface parameters and constants remained the same as those reported for the pure ferric oxyhydroxide suspensions (Table 2). In the model, it was assumed that all of the iron in the suspension was in the form of FeOOH(am) under oxic conditions. Because As in the source water was removed by coagulation with ferric chloride, FeOOH(am) was considered to be the principal adsorbent for As in the suspension.

The adsorption isotherms and the best-fit curves obtained by MINTEQA2 (*24*) are plotted in Figure 2. The isotherms were obtained by adding different amounts of As(V) and As(III) separately to fresh S-2 sample and measuring the equilibrium concentration of As(V) and As(III) after 24 h of mixing. The best-fit curves described the As(III) and As(V) isotherms reasonably well. Adsorption reactions 1 and 2 in Table 2 were used to calculate the adsorption of As(V) and As(III). The best-fit constants determined for the surface complexes $Fe-AsO_4^{2-}$ and $Fe-HAsO_3^-$ were $10^{-2.3}$ and $10^{-3.3}$, respectively. These were conditional adsorption constants for the backwash suspension which accounted for the adverse effects of anions such as silicate (*21*) and the interactions among the multicomponent solids such as ferric oxyhydroxide and other inorganic and organic particles (*27*).

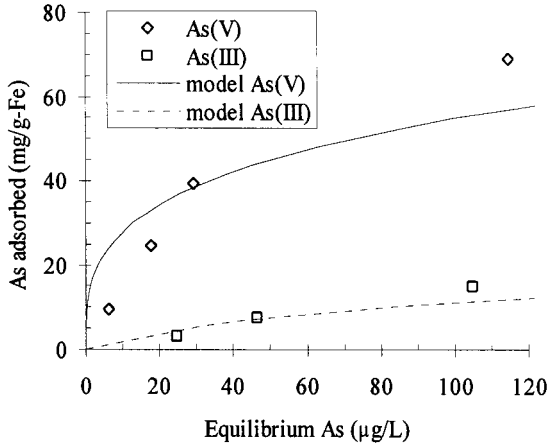

FIGURE 2. Model simulation of As(V) and As(III) adsorption isotherms in fresh Suspension 2 (S-2) sample. Equilibrium pH = 7.0; total FeOOH(am) = 1.04 g/L.

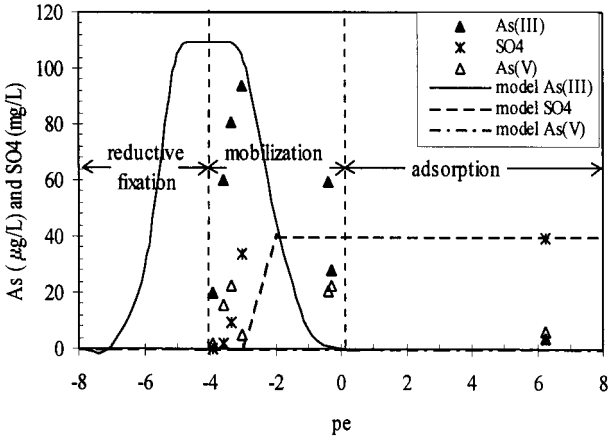

FIGURE 3. Experimental and predicted soluble concentrations of As(III), SO_4^{2-}, and As(V) as a function of pe during aging of Suspension 2 (S-2) sample in a closed system. pH range 6.98−7.76.

The best-fit adsorption constants and the thermodynamic equilibrium constants were subsequently used to predict the transformations of As, S, and Fe during the aging of S-2 sample. The model calculations considered adsorption of As(III) and As(V) species, reduction of As(V) to As(III), SO_4^{2-} to HS^-, and precipitation of orpiment (As_2S_3), realgar (AsS), arsenopyrite (FeAsS), and pyrite (FeS). The initial concentrations of Fe, As, SO_4^{2-}, and HCO_3^- in the model suspension, chemical reactions, and the equilibrium constants used in the model calculations are reported in Table 2. The model system was closed to the atmosphere because the suspension samples were isolated from atmospheric air in the aging tests.

The experimental and predicted soluble concentrations of As(III), As(V), and SO_4^{2-} in the S-2 sample are plotted as a function of pe in Figure 3. Figure 4 shows the predicted distribution of As and S and the experimental FeOOH(am) in the solid phase. This figure is used to illustrate the transformations of As and Fe in the solid phase and the release of arsenic from the solid phase to the liquid phase. The soluble arsenic concentrations were below 10 μg/L at low and high pe values and were higher than 10 μg/L in the intermediate pe range (Figure 3). On the basis of the observed mobility of arsenic, the pe range could be divided into three redox zones: defined as adsorption, mobilization, and reductive fixation zones. The adsorption zone at pe > 0 was characterized by the presence of stable As(V) and FeOOH(am) forms. As(V) was immobilized through adsorption on FeOOH(am) (Figure 4).

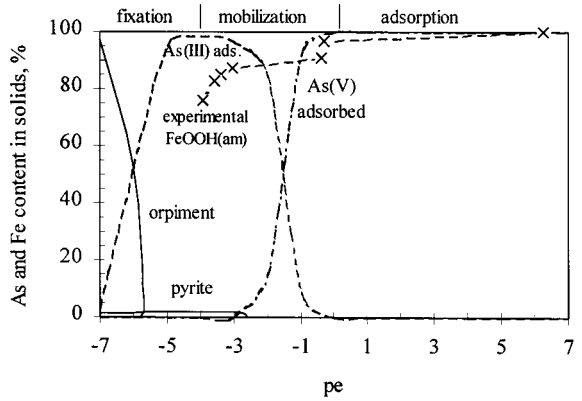

FIGURE 4. Model predictions of the transformations of As and Fe in the solid phase. "Experimental FeOOH(am)" denotes the observed FeOOH(am) content used in the model calculations.

The pe of the mobilization or transition zone was between 0 and −4.0 where reduction of As(V) and FeOOH(am) occurred and some of the As(III) and As(V) were released to the liquid phase. This is a transitional range between the oxidized solid phase [i.e., FeOOH(am)] and the reduced solid phase such as pyrite and arsenic pyrite (Figure 4). As(III) and As(V) concentrations increased from less than 5 μg/L at pe 6.3 to 94 and 22 μg/L, respectively, at pe of approximately −3. The maximum soluble As(III) concentration was much lower than that obtained in the S-1 sample (Figure 1), which is due to lower total arsenic content in the S-2 sample (Table 1). Similar effects of redox potential have been observed in reservoir sediment (*28*). When the pe values of the sediment decreased from 0 to −3.4, the total soluble arsenic concentration increased by approximately 25 times.

The dramatic decrease in SO_4^{2-} concentration at pe of approximately −3.0 can be attributed to the reduction of SO_4^{2-} to sulfide (Figure 3). Subsequently, the sulfide forms pyrite with the Fe(II) generated through the reduction of FeOOH(am) (Figure 4). The concurrent decrease in the concentrations of As(III), As(V), and SO_4^{2-} in a narrow pe range between −3.0 and −4.0 indicated that the As species were immobilized by sulfide minerals and other reduced solid phases. Therefore, the pe < −4.0 range is defined as the reductive fixation zone. Edwards (*29*) has predicted the conversion of adsorbed arsenic species in aerobic environment into co-precipitates with FeS under anoxic conditions.

The SO_4^{2-} profile predicted by the model was similar to that observed experimentally (Figure 3). According to thermodynamic predictions, the reduction of SO_4^{2-} was initiated at pe of approximately −2.0 in contrast to the observed SO_4^{2-} reduction pe of approximately −3.0. This discrepancy could be attributed to the relatively low reduction rate of SO_4^{2-}. During the first 22 days of aging the pe decreased continuously from 6.3 to −3.9. If the redox reactions proceeded more slowly than the rate of pe decrease mediated by biological activity, the observed concentrations of SO_4^{2-} and other redox-sensitive chemical species such as As(V) and Fe(III) would not be equal to the equilibrium values with respect to the measured pe. Furthermore, because many redox processes do not couple with each other readily, it is possible to have several different oxidation−reduction levels for different species in the same system (*30*).

The calculated As(III) line also shows a soluble As(III) peak near the mobilization zone in Figure 3. However, the predicted As-release zone is shifted toward the lower pe region by approximately two pe units as compared with the experimental data. The higher pe boundary of the predicted arsenic peak was defined by several factors, including the reductive formation of As(III), the adsorption of As(III), and the reductive dissolution of FeOOH(am). The difference

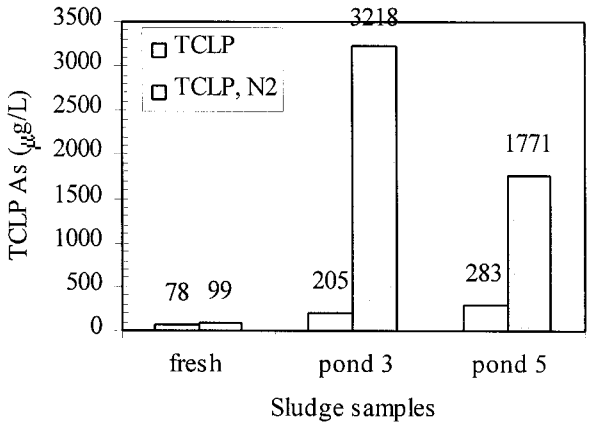

FIGURE 5. Leachability of As determined by TCLP and modified TCLP (i.e. TCLP, N_2). V_a/V_L ratio = 0.5.

between the predicted and observed release of As in the higher pe range could be attributed to the nonequilibrium conditions in the suspension.

Modeling results indicated that the lower pe boundary of the predicted As peak (Figure 3) was resulted from the precipitation of As(III) with sulfide as orpiment. Thermodynamic calculations predicted the formation of orpiment at pe < −5.5 and the precipitation of pyrite at pe < −2.7 (Figure 4). Only 1.74% of the total Fe formed pyrite because of the limited amount of sulfide in the suspension (i.e. S = 0.417 mM). It is possible that the observed decrease in soluble As(III) at pe of approximately −3.0 was caused by association of the As(III) with the pyrite rather than by the formation of orpiment. In anoxic environments, arsenic-rich pyrite (arsanian pyrite) is commonly present in sediments and soils (*14*, *31*−*33*). Arsenic can be associated with pyrite through inclusion and isomorphic substitution. The arsenic content in natural arsenic-rich pyrite varies from less than 0.5 to 8% (*34*), which is substantially less than its content in arsenic sulfide minerals such as orpiment and arsenopyrite.

If the reduction of Fe(III) to Fe(II) were to reach equilibrium, all of the FeOOH(am) would be dissolved and most of the As would be released (total As = 6380 μg/L) to the liquid phase, resulting in a very high soluble arsenic peak at pe = −4.0 (the calculated data are not presented in Figure 3). In fact, less than 25% of the total Fe in the aged suspension was converted to Fe(II) due to the slow reduction rate. The actual ferric oxyhydroxide content measured in the suspension was used to calculate the adsorption of As(V) and As(III).

The model failed to predict the release of As(V) in the mobilization zone (Figure 3). According to the modeling predictions, the soluble As(V) concentration should be less than 1 μg/L in the pe range studied. In the suspension, As(V) was released during the reductive dissolution of ferric oxyhydroxide. The high As(V) concentration observed in the mobilization zone could be caused by a slow reduction of As(V) to As(III). A small fraction of As(V) usually exists in groundwater and mine tailings porewater under anoxic conditions (*14*, *35*).

Effects of DO on TCLP Leachability. When the backwash suspension was discharged and cumulated in the ponds, it was converted into anoxic sludge. The sludge samples had a dark color and a foul smell. Speciation analysis indicated that approximately 38 and 57% of the total Fe in Ponds 3 and 5 sludge samples, respectively, was in extractable Fe(II) form (Table 1). When the samples were tested with the TCLP, 205 and 283 μg/L As was extracted from the Ponds 3 and 5 sludge samples, respectively (Figure 5). The V_a/V_L ratio in the extraction vessels was 0.5. When the mixtures of sludge and the TCLP leachant were purged for 15 min and then tumbled

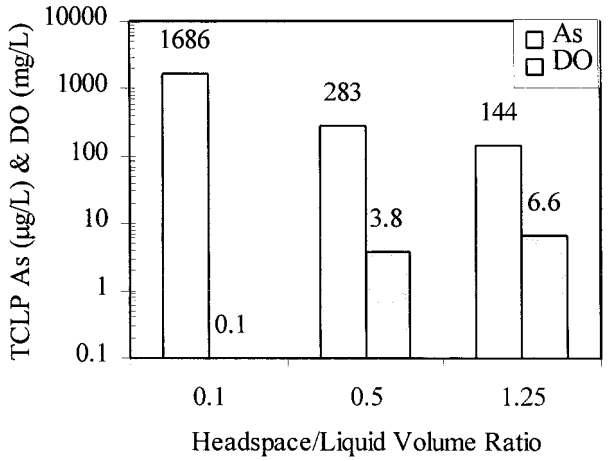

FIGURE 6. Effects of V_a/V_L ratios on the leachability of arsenic determined by TCLP, Pond 5 sludge sample.

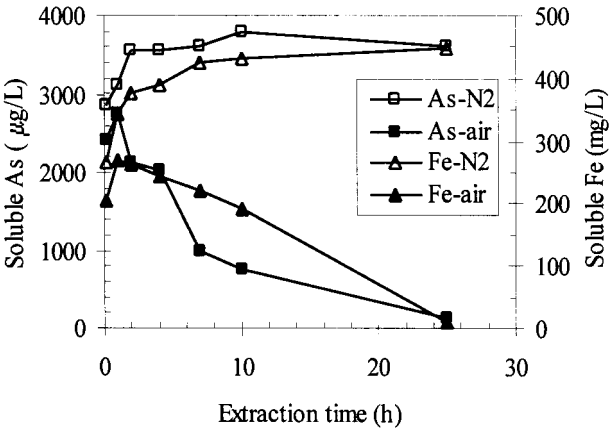

FIGURE 7. Variations of soluble As and Fe concentrations with time in kinetic extraction tests. Pond 3 sludge sample.

for extraction, the leachate As concentrations increased to 3218 μg/L and 1771 μg/L. These concentrations are close to the current TCLP limit (i.e., 5000 μg/L) for hazardous material. The amounts of As extracted from the fresh sludge sample by the TCLP and the modified TCLP were 78 and 99 μg/L, respectively. The results show that the presence of oxygen in the extraction vessels dramatically decreased the leachability of arsenic in the anoxic sludge samples. On the other hand, the leachability of As in the oxic sludge was not affected much by the presence of oxygen. The final pH of the leachate was between 5.1 and 5.3.

The effect of oxygen on the TCLP results was further evaluated by varying the V_a/V_L ratio in TCLP tests. When the V_a/V_L ratio was increased from 0.1 to 1.25, the As concentration in the leachate decreased from 1686 μg/L to 144 μg/L (Figure 6). The final DO content in the extraction solutions increased from less than 0.1 mg/L to 6.6 mg/L when the V_a/V_L ratio increased from 0.1 to 1.25. Similar leaching results were obtained when the Pond 5 sample was extracted at V_a/V_L = 0.1 (Figure 6) and in the N_2 purged system (Figure 5). In the presence of DO, the TCLP dramatically underestimates the leachability of As in the anoxic sludge. The use of extraction vessels with different sizes may result in large variations in the TCLP results.

Figure 7 shows the changes in total soluble As and Fe concentrations obtained from the kinetic extraction experiment. When the extraction was performed under a nitrogen atmosphere, the soluble As and Fe concentrations increased gradually to approximately 3600 μg/L and 430 mg/L, respectively, during the first 10 h of extraction and remained

constant thereafter. When the extraction was performed in air, the soluble As and Fe concentrations increased to approximately 2800 μg/L and 270 mg/L within 1 h. Both As and Fe concentrations decreased dramatically when the extraction time was extended from 1 to 25 h. More than 90% of the soluble As in the air- and N_2-purged systems was in the As(III) form because most of the As(V) was adsorbed by ferric oxyhydroxide.

The decrease in Fe concentrations during the extraction in air was due to the oxidation of ferrous ion and subsequent precipitation of ferric oxyhydroxide. The soluble As(V) and As(III) could be removed by the newly formed ferric oxyhydroxide. During the TCLP extraction in the presence of DO, some of the As(III) might also undergo oxidation to As(V) and be subsequently removed by the ferric oxyhydroxide. Rapid oxidation of geothermal As(III) has been observed in streamwaters (*36*).

Environmental Implications. Elevated arsenic concentrations in groundwater have been attributed to the reduction of iron oxyhydroxide (*37*) and the oxidation of arsenic-rich pyrite and other reduced minerals (*31*, *33*). The modeling and experimental results suggest that arsenic release occurs in an intermediate pe range (i.e., $-4.0 < pe < 0$) where the transformations between the reduced and oxidized solid phases take place. In natural systems, the boundaries of the mobilization zone may shift to lower or higher pe ranges depending on the reduction or oxidation reactions, the types of minerals responsible for the immobilization of arsenic, and the reaction kinetics. At $pe < -4$, high sulfur and Fe contents in the sediments may enhance the immobilization of arsenic through the formation of arsenic-rich pyrite. The sludge generated during the treatment of surface water becomes rapidly anoxic because of its high TOC content and high microbial mass. If a filtration run is interrupted for a few days, substantial amounts of soluble As(III) and Fe(II) may form in the idle filters. To prevent the release of high As(III) concentrations into the water supply system, the filters should be flushed or backwashed before the filtration is resumed.

Acknowledgments

The work was supported partly by the New Jersey Department of Environmental Protection. The authors thank Robert T. Mueller and Michael Winka of NJDEP for their support; Don Christie, Gary F. Stolarik, and Mark J. Sedlacek for assistance with sample collection at the plant; and Mahmoud Wazne and Sunbaek Bang for assistance with laboratory experiments.

Literature Cited

(1) Cheng, R. C.; Liang, S.; Wang, H. C.; Beuhler, M. D. *J.−Am. Water Works Assoc.* **1994**, *86* (9), 79−90.
(2) McNeill, L. S.; Edwards, M. *J.−Am. Water Works Assoc.* **1995**, *87* (4), 105−113.
(3) Hering, J. G.; Chen, P. Y.; Wilkie, J. A.; Elimelech, M.; Liang, S. *J.−Am. Water Works Assoc.* **1996**, *88* (4), 155−167.
(4) Hogue, C. *Chem. Eng. News* **2001**, *79* (21), 51−55.
(5) Frey, M. M.; Owen, D. M.; Chowdhury, Z. K.; Raucher, R. S.; Edwards, M. A. *J.−Am. Water Works Assoc.* **1998**, *90* (3), 89−102.
(6) Korte, N. E.; Fernando, Q. *Crit. Rev. Environ. Control* **1991**, *21*, 1−39.
(7) Ahmann, D.; Krumholz, L. R.; Lovley, D. R.; Morel, F. R. R. *Environ. Sci. Technol.* **1997**, *31*, 2923−2931.
(8) Harrington, J. M.; Fendorf, S. E.; Rosenzweig, F. R. *Environ. Sci. Technol.* **1998**, *32*, 2425−2430.
(9) Moore, J. N.; Ficklin, W. H.; Johns, C. *Environ. Sci. Technol.* **1988**, *22*, 432−437.
(10) Cummings, D. E.; Caccavo, F., Jr.; Fendorf, S.; Rosenzweig, F. G. *Environ. Sci. Technol.* **1999**, *33*, 723−729.
(11) Kuhn, A.; Sigg, L. *Limnol. Oceanogr.* **1993**, *38*, 1052−1059.
(12) Spliethoff, H.; Mason, R. P.; Hemond, H. F. *Environ. Sci. Technol.* **1995**, *29*, 2157−2161.
(13) Rochette, E. A.; Bostick, B. C.; Li, G. C.; Fendorf, S. *Environ. Sci. Technol.* **2000**, *34*, 4714−4720.
(14) McCreadie, H. J.; Blowes, D. W.; Ptacek, C.; Jambor, J. L. *Environ. Sci. Technol.* **2000**, *34*, 3159−3166.
(15) U.S. Environmental Protection Agency. *Test Methods for Evaluating Solid Waste, Physical/Chemical Methods*, 3rd edition; SW-846, Method 1311; U. S. Government Printing Office: Washington, DC, 1992.
(16) Hooper, K.; Iskander, M.; Sivia, G.; Hussein, F.; Hsu, J.; Deguzman, M.; Odion, Z.; Ilejay, Z.; Sy, F.; Petreas, M.; Simmons, B. *Environ. Sci. Technol.* **1998**, *32*, 3825−3830.
(17) Stolarik, G. F.; Christie, J. D. *Proceedings of the 1999 American Water Works Association Annual Conference*; Chicago, IL, June 20−24, 1999; AWWA: Washington, DC, 1999.
(18) Kneebone, P. E.; Hering, J. G. *Environ. Sci. Technol.* **2000**, *34*, 4307−4312.
(19) U.S. Environmental Protection Agency. *Test Methods for Evaluating Solid Waste, Physical/Chemical Methods*, 3rd edition; SW-846, Method 3050B; U.S. Government Printing Office: Washington, DC, 1992.
(20) Meng, X. G.; Wang, W. Speciation of Arsenic by Disposable Cartridges. In *Book of Posters of the Third International Conference on Arsenic Exposure and Health Effects*; Society of Environmental Geochemistry and Health, University of Colorado at Denver: Denver, CO, 1998.
(21) Meng, X. G.; Bang, S. B.; Korfiatis, G. P. *Wat. Res.* **2000**, *34*, 1255−1261.
(22) Ye, M. Y.; Shen, Y., West, C. C.; Lyon, W. G. *J. Liq. Chromatogr. Relat. Technol.* **1998**, *21*, 551−565,
(23) Clesceri, L. S.; Greenberg, A. E.; Trussell, R. R.; Franson, M. A. *Standard Methods for the Examination of Water and Wastewater*, 20th edition; Method 3500-Fe B; American Public Health Association: Washington, DC, 1998.
(24) David, S. B.; Allison, J. D. *MINTEQA2, An Equilibrium Metal Speciation Model: User's Manual 4.01*; Environmental Research Laboratory, US Environmental Protection Agency: Athens, GA, 1999.
(25) Barrow, N. J.; Bowden, J. W. *J. Colloid Interface Sci.* **1987**, *119*, 236−250.
(26) Dzombak, D. A.; Hayes, K. F. *Environ. Sci. Technol.* **1992**, *26*, 1253−1254.
(27) Meng, X. G.; Letterman, R. D. *Environ. Sci. Technol.* **1993**, *27*, 970−975.
(28) Masscheleyn, P. H.; Delaune, R. D.; Patrick, W. H., Jr. *J. Environ. Qual.* **1991**, *20*, 522−527.
(29) Edwards, M. *J.−Am. Water Works Assoc.* **1994**, *86* (9), 64−78.
(30) Stumm, W.; Morgan, J. J. *Aquatic Chemistry*, 2nd ed.; John Wiley & Sons Inc.: New York, 1981; pp 418, 241.
(31) Peters, S. C.; Blum, J. D.; Klaue, B.; Karagas, M. R. *Environ. Sci. Technol.* **1999**, *33*, 1328−1333.
(32) Simon, G.; Huang, H.; Penner-Hahn, J. E.; Kesler, S. E.; Kao, L. S. *Am. Mineral.* **1999**, *84*, 1071−1079.
(33) Kim, M. J.; Nriagu, J.; Haack, S. *Environ. Sci. Technol.* **2000**, *34*, 3094−3100.
(34) Fleet, M. E.; Chryssoulis, S. L.; MacLean, P. J.; Davidson, R.; Weisener, C. G. *Can. Mineral.* **1993**, *31*, 1−17.
(35) Meng, X. G.; Korfiatis, G. P.; Christodoulatos, C.; Bang, S. B. *Wat. Res.* **2001**, *35*, 2805−2810.
(36) Wilkie, J. A.; Hering, J. G. *Environ. Sci. Technol.* **1998**, *32*, 657−662.
(37) Nickson, R.; McArthur, J.; Burgess, W. G.; Ahmed, K. M.; Ravenscroft, P.; Rahman, M. *Nature* **1998**, *395*, 338.

Received for review February 14, 2001. Revised manuscript received June 9, 2001. Accepted June 13, 2001.

ES010645E